Journal for ImmunoTherapy of Cancer

Intratumoral and peritumoral radiomics of MRIs predicts pathologic complete response to neoadjuvant chemoimmunotherapy in patients with head and neck squamous cell carcinoma

Peiliang Lin ,[1,2] Wenqian Xie,[1,2] Yong Li,[1,3] Chenjia Zhang,[1,2] Huiqian Wu,[1,4] Huan Wan,[1,5] Ming Gao,[1,3] Faya Liang,[1,2] Ping Han ,[1,2] Renhui Chen,[1,2] Gui Cheng,[6] Xuekui Liu,[7] Song Fan,[1,8] Xiaoming Huang [1,2]

To cite: Lin P, Xie W, Li Y, *et al*. Intratumoral and peritumoral radiomics of MRIs predicts pathologic complete response to neoadjuvant chemoimmunotherapy in patients with head and neck squamous cell carcinoma. *Journal for ImmunoTherapy of Cancer* 2024;**12**:e009616. doi:10.1136/jitc-2024-009616

► Additional supplemental material is published online only. To view, please visit the journal online (https://doi.org/10.1136/jitc-2024-009616).

PL, WX and YL contributed equally.

Accepted 01 October 2024

For numbered affiliations see end of article.

Correspondence to
Professor Xiaoming Huang; hxming@mail.sysu.edu.cn

Professor Song Fan; fansong2@mail.sysu.edu.cn

Professor Xuekui Liu; liuxk@sysucc.org.cn

ABSTRACT

Background For patients with locally advanced head and neck squamous cell carcinoma (HNSCC), combined programmed death receptor-1 inhibitor and chemotherapy improved response rate to neoadjuvant therapy. However, treatment response varies among patients. There is no tool to predict pathologic complete response (pCR) with high accuracy for now. To develop a tool based on radiomics features of MRI to predict pCR to neoadjuvant chemoimmunotherapy (NACI) may provide valuable assistance in treatment regimen determination for HNSCC.

Methods From January 2021 to April 2024, a total of 172 patients with HNSCC from three medical center, who received NACI followed by surgery, were included and allocated into a training set (n=84), an internal validation set (n=37) and an external validation set (n=51). Radiomics features were extracted from intratumoral and different peritumoral areas, and radiomics signature (Rad-score) for each area was constructed. A radiomics-clinical nomogram was developed based on Rad-scores and clinicopathological characteristics, tested in the validation sets, and compared with clinical nomogram and combined positive score (CPS) in predicting pCR.

Results The radiomics-clinical nomogram, incorporating peritumoral Rad-score, intratumoral Rad-score and CPS, achieved the highest accuracy with areas under the receiver operating characteristic curve of 0.904 (95% CI, 0.835 to 0.972) in the training cohort, 0.860 (95% CI, 0.722 to 0.998) in the internal validation cohort, and 0.849 (95% CI, 0.739 to 0.959) in the external validation cohort, respectively, which outperformed the clinical nomogram and CPS in predict pCR to NACI for HNSCC.

Conclusion A nomogram developed based on intratumoral and peritumoral MRI radiomics features outperformed CPS, a widely employed biomarker, in predict pCR to NACI for HNSCC, which would provide incremental value in treatment regimen determination.

WHAT IS ALREADY KNOWN ON THIS TOPIC

⇒ Neoadjuvant chemoimmunotherapy (NACI), combining traditional chemotherapy with an anti-programmed death receptor-1 antibody, has shown promising outcomes for treating head and neck squamous cell carcinoma (HNSCC), as reported in recent studies. However, patient responses to NACI vary significantly. To date, no highly accurate tool exists to predict NACI responses in HNSCC.

WHAT THIS STUDY ADDS

⇒ To our knowledge, this is the first multicenter study employing both intratumoral and peritumoral radiomics features derived from pretreatment MR images to predict the response to NACI in HNSCC, offering valuable biological insights. The non-invasive biomarker developed in this study surpasses the widely used combined positive score (CPS) in predicting NACI for HNSCC. It also shows a correlation with the density of tumor-infiltrating lymphocytes and fibroblasts in both intratumoral and peritumoral areas.

HOW THIS STUDY MIGHT AFFECT RESEARCH, PRACTICE, OR POLICY

⇒ The study underscores that the non-invasive MRI biomarker provides enhanced predictive accuracy for NACI response in HNSCC over the currently used CPS biomarker. The adoption of this non-invasive approach could potentially improve functional preservation and facilitate the implementation of treatment de-escalation strategies for patients with HNSCC.

INTRODUCTION

Worldwide, head and neck squamous cell carcinoma (HNSCC) is one of the most common malignancies, with over 500,000 new cases reported annually.[1–3] Approximately, 60% of patients with HNSCC are diagnosed with locally advanced disease.[1] The patients with locally advanced HNSCC are treated with either extensive surgical resection followed by adjuvant (chemo)radiotherapy,

or definitive concurrent chemoradiotherapy. Still, the 5-year overall survival (OS) of HNSCC is only 40–53%, even at the expense of function damage, such as speech pronunciation, swallowing, or esthetics.[4]

Immunotherapy is an emerging field in malignance treatment in recent years. In 2019, KEYNOTE-048 trial showed that compared with cetuximab plus chemotherapy, pembrolizumab with or without chemotherapy (for tumors with combined positive score (CPS)≥1) improved OS for recurrent/metastatic (R/M) HNSCC.[5] Pembrolizumab alone (for tumors with CPS≥1), or pembrolizumab with chemotherapy, has been established for first-line treatment of recurrent/metastatic HNSCC.[6] Compared with R/M HNSCC, the better immune status of patients and fewer drug-resistant clones make the patients more responsive to neoadjuvant immunotherapy or chemoimmunotherapy. Recently, several published trials of neoadjuvant immunotherapy or chemoimmunotherapy in HNSCC reported promising results.[7–9] With neoadjuvant chemoimmunotherapy (NACI), the patients achieved about 36.4%~42.0% of pathologic complete response (pCR), an indicator of better prognosis being recognized in several trials, which may lay the foundation of treatment de-escalation and function preservation.[9–13] However, not all patients showed much responsiveness to neoadjuvant chemoimmunotherapy. For these patients, neoadjuvant chemoimmunotherapy increased the incidence of complications, even delayed surgery without prognosis improvement.[14]

Now, there is a desideration of an accurate and non-invasive method to predict the response of HNSCC to neoadjuvant chemoimmunotherapy. The widely employed biomarkers, such as CPS, tumor cell proportion score and immune cell proportion score, were not sufficient to predict the efficacy of the combination therapy above.[15 16] Radiomics is a rapidly evolving technique to transform medical images into high-throughput and quantifiable data.[17 18] The predefined algorithms could extract intricate features from medical image, reflecting details not only about the overall tumor burden but also tumor heterogeneity.[18 19]Intratumoral radiomics was proved to be useful to predict response to neoadjuvant chemoimmunotherapy in some other cancers.[20 21] However, peritumoral area plays an important role in tumor immune interaction. The radiomic features of peritumoral area may infer tumor-associated microenvironment status and predict response to chemoimmunotherapy.[22]

Therefore, the aim of our study was to develop and validate a nomogram based on intratumoral and peritumoral radiomics to predict the response to neoadjuvant chemoimmunotherapy in HNSCC.

METHOD

Patients

This retrospective analysis of anonymous data was approved by the ethics committee with a waiver of informed consent (SYSKY-2023-1175-01). Patients with HNSCC, who were treated in Sun Yat-sen Memorial Hospital between January 2021 and February 2023, were included and randomly allocated into a training set (n=84) and an internal validation set (n=37). Patients treated in Sun Yat-sen University Cancer Center and Shenshan Medical Center, Memorial Hospital of Sun Yat-sen University between April 2021 and April 2024, were assigned as an external validation set (n=51) (online supplemental figure 1). The inclusion criteria were as follows: (1) patients pathologically diagnosed with HNSCC; (2) patients receiving two or three courses of neoadjuvant therapy (traditional chemotherapy plus programmed death receptor-1 (PD-1 inhibitor); (3) MR scan within 30 days before the first course of neoadjuvant therapy; (4) patients undergoing radical surgical dissection following neoadjuvant therapy; (5) complete clinical data available. The exclusion criteria were as follows: (1) previous head and neck treatment history; (2) obvious motion or metal artifacts on the MRI image; (3) distant metastasis; (4) concurrent malignancies.

Baseline clinical data, such as age, gender, tobacco consumption, alcohol consumption and so on, were derived from medical records. All MR images were reviewed and annotated by two radiologists with 15 years and 10 years, who were both experienced in interpreting head and neck MRI. All pathological assessments were performed by two expert pathologists independently, who were blind to other clinical information of the patients.

Imaging acquisition, region-of-interest segmentation and radiomic feature extraction

The patients included in the study underwent head and neck MRI scans using a 1.5 Tesla MR scanner (Magnetom Avanto, Siemens Medical Solutions, Erlangen, Germany) at Sun Yat-sen Memorial Hospital, a 1.5 Tesla MR scanner (GE Signa Voyage, GE Healthcare, Chicago, USA) at Shenshan Medical Center, Memorial Hospital of Sun Yat-sen University, or a 3.0 Tesla MR scanner (Achieva, Philips Healthcare, the Netherlands) at the Sun Yat-sen University Cancer Center. The acquisition sequences included axial oblique T2-weighted imaging and contrast-enhanced T1-weighted with fat suppression imaging. The first step involved z-score normalization of the raw image stacks for subsequent feature extraction. The whole tumor was manually delineated slice-by-slice by a radiologist with 10 years of experience in head and neck cancer imaging and then confirmed by an experienced radiologist with 15 years on the ITK-SANP platform (V.3.8, www.itksnap.org). Morphological operations were conducted on these annotated regions within each slice to create peritumor areas. Image dilation expanded the tumor areas to generate outer peritumor areas, while image erosion shrank the tumor areas to yield inner peritumor areas. Annular 3 mm wide areas at a radial distance of −3 mm (inside) to 9 mm (outside) from the edge of the segmented region were created finally. Peritumoral areas were obtained with varying widths. Subsequently, interpolation was employed on all DICOM images and

corresponding masks of tumors and peritumoral areas to standardize spatial resolution along the XYZ directions.

A total of 2608 conventional radiomics features were extracted from each intratumoral or peritumoral area. Radiomics feature extraction used the PyRadiomics toolkit (V.3.0.1), implemented in Python (V.3.8.3), with details summarized in online supplemental table 1.[23]

Feature selection and radiomics signature construction

The intraobserver and interobserver reproducibility of radiomics feature extraction were assessed by intraclass and interclass correlation coefficients (ICCs). Initially, we randomly chose 30 cases for region of interest (ROI) segmentation and feature extraction of MR images. Two radiologists, 1 with 10 years of experience and the other with 15 years of experience in interpreting head and neck MR images, independently performed the ROI delineation. Reader 1 then repeated the same procedure 1 week later. An ICC value exceeding 0.75 indicates a high level of concordance in the feature extraction process, and radiomics features with ICC<0.75 were excluded.

The remaining radiomics features were reserved and further selected using the least absolute shrinkage and selection operator (LASSO) method. A formula generated by a linear combination was determined by the weighted LASSO coefficients. This formula was used to compute risk scores based on selected radiomics features extracted from intratumoral or different peritumoral areas, referred to as the radiomics scores (Rad-scores) (figure 1). The scores served as quantitative indicators of the likelihood of achieving pCR.

Construction of the radiomics-clinical nomogram

The Rad-scores computed based on radiomics features extracted from different peritumoral areas were compared with determine the best peritumoral Rad-score according to the area under receiver operator characteristic curve (ROC) in predicting pCR for HNSCC. The best peritumoral Rad-score, intratumoral Rad-score and clinical candidate predictors (ie, age, sex, CPS) were tested in a univariate logistic regression algorithm in the training dataset. A multivariate logistic regression algorithm was applied to identify the independent predictors. The collinearity diagnosis of the multivariate logistic regression was performed using the variance inflation factor (VIF). Subsequently, a radiomics-clinical nomogram (radiomics-clinical nomogram II) was developed using the results of the multivariate logistic analysis, with the aim to assess the individual probability of pCR in the training dataset. At the same time, another radiomics-clinical nomogram (radiomics-clinical nomogram I) was developed based on intra-Rad-score and clinicopathological characteristics, and a clinical one (clinical nomogram) was based on clinical independent predictors.

Validation of the radiomics-clinical nomogram performance

The predictive performance of the radiomics-clinical nomogram was validated in the internal and external validation datasets. In the validation sets, the radiomics scores were calculated for each patient using the formula derived from the training set. The discriminatory power of the radiomics-clinical nomogram was quantified by calculating the area under the curve (AUC) for the training set, as well as for both the internal and external validation sets, respectively. Calibration curves were used to assess the calibration of the nomogram at the same time.

Assessment of the radiomics-clinical nomogram

To assess the clinical utility of the radiomics-clinical nomogram, a decision curve analysis (DCA) was performed, which involved the calculation of net benefits across various threshold probabilities in the combined training and validation set. The AUC of radiomics-clinical nomogram II was compared with the performance of radiomics-clinical nomogram I, clinical nomogram, Rad-scores, and CPS at the same time.

Model interpretability

Biopsy sample obtained before neoadjuvant therapy were available for a subset of patients from Sun Yat-sen Memorial Hospital. H&E stained whole-slide tissue scans analysis was performed to explore how each radiomics feature and the integrated radiomics signatures influenced the model prediction for the response to neoadjuvant chemoimmunotherapy in HNSCC. The cell detection and classification process were facilitated by the QuPath open-source software platform. For each slice, six random 250 micron by 250 micron fields were selected from the intratumoral area, and an additional six fields were chosen from the peritumoral area of −3 to 0 mm. Tumor-infiltrating lymphocytes (TILs) were indicated to be associated with prognosis in HNSCC.[24] Cells detected in both the intratumoral and peritumoral regions were categorized by two pathologists into four groups: tumor cells, immune cells, fibroblasts, and other detections (online supplemental figure 2). Cells densities and immune cell ratios were calculated, which included total cell density, tumor cell density, immune cell density, fibroblast density, esTILs% (stromal TILs percentage), etTILs% (total TILs percentage) and eTILs% (enhanced TILs percentage). The formulas for these percentages are shown below:

1. esTILs% = 100 × (immune cell density / (stromal cells density = total cell density − tumor cell density))
2. etTILs% = 100 × (immune cell density / total cell density)
3. eTILs% = 100 × (immune cell density / (immune cell density + tumor cell density))

Interobserver agreement was assessed using ICC of total cell density, tumor cell density, immune cell density, and fibroblast density. The tissue scan would be reviewed, and cells detected would be reclassified by the pathologists when ICC was below 0.75. Otherwise, the average values determined by both pathologists would be used for subsequent analysis. The correlation between pathologic variables and radiomics features was assessed to explore

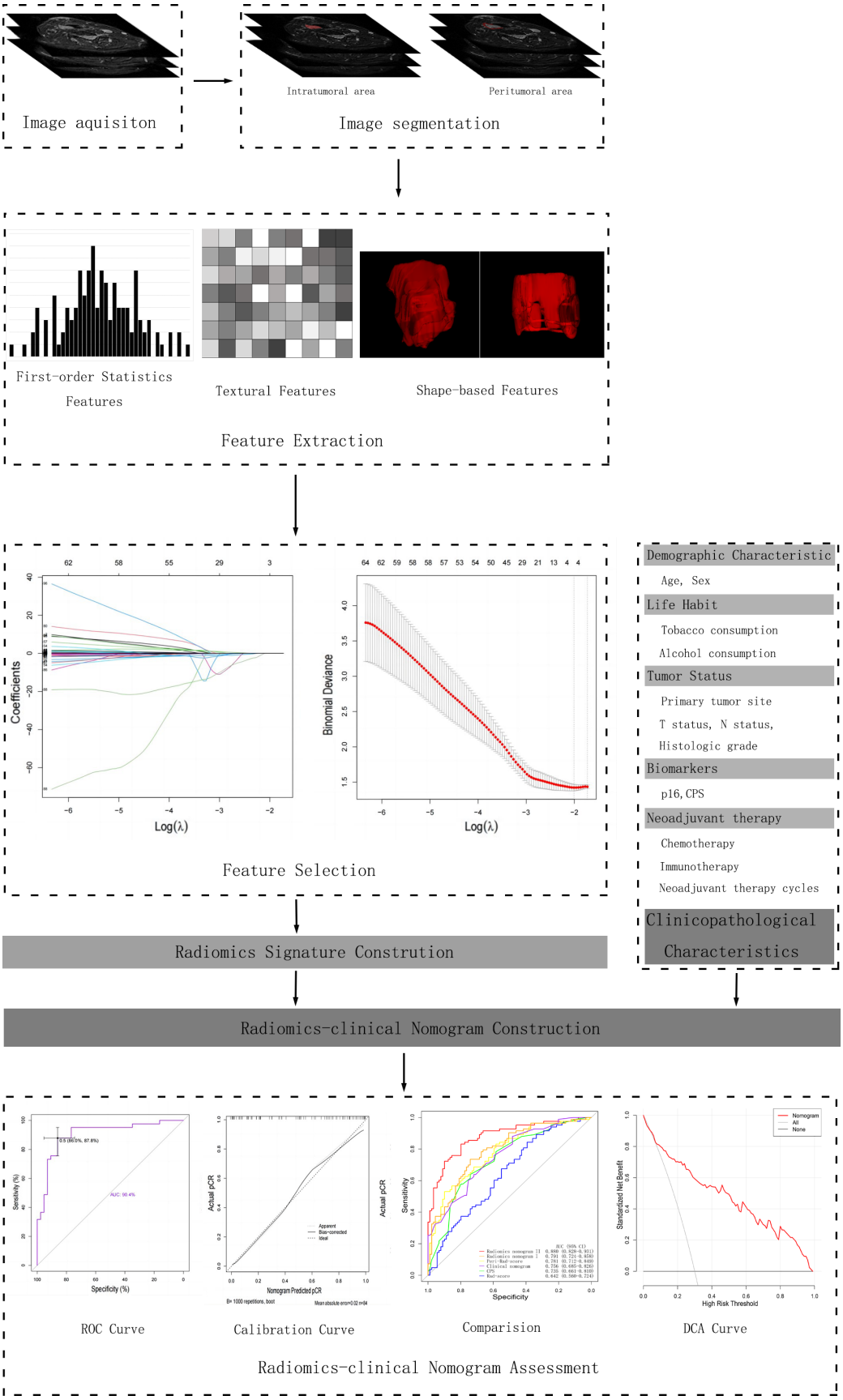

Figure 1 The workflow for the development of the radiomics-clinical nomogram to predict pathologic complete response to neoadjuvant chemoimmunotherapy in head and neck squamous cell carcinoma. AUC, area under the receiver operator characteristic curve; CPS, combined positive score; DCA, decision curve analysis; pCR, pathologic complete response; ROC, receiver operator characteristic curve.

whether the radiomics features could potentially capture information about TILs on MRI scans.

Statistical analysis

All statistical analyses were performed by R statistical software (V.4.2.1) and SPSS software (V.26.0, Chicago, Illinois, USA). A two-sided p value<0.05 was considered the statistical significance threshold. The statistical differences were compared using χ^2 test or Fisher exact test for categorical variables and the Kruskal-Wallis test for numeric clinicopathological variables. The association between two quantitative variables was assessed using Pearson correlation analysis.

In this study, the "glmnet" package was used for LASSO logistic regression. The diagnostic ability of predictive pCR was evaluated by the ROC curves. The "pROC" package was plotted for the ROC curve. The "rms" package was used for nomogram construction and calibration plots. DCA was performed using the "dca.R".

RESULT

Clinicopathologic characteristics of cohorts

A total of 277 patients with HNSCC receiving neoadjuvant chemoimmunotherapy in Sun Yat-sen Memorial Hospital were identified, whom 121 patients were screened out among according to the inclusion and exclusion criteria. The patients were randomly assigned to a training set (n=84) and an internal validation set (n=37). 131 patients with non-recurrent HNSCC and complete clinical data, who received neoadjuvant chemoimmunotherapy and radical surgery in Sun Yat-sen University Cancer Center and Shenshan Medical Center, Memorial Hospital of Sun Yat-sen University between April 2021 and April 2024, were identified, and 51 patients were included finally as an external validation set (online supplemental figure 1). The patients' baseline characteristics are shown in table 1. The age (mean±SD) of all the patients was 54.6±11.9 years old. 133 (77.3%) of them were men, and 39 (22.7%) were women. The majority of them were stage III/IV. Over 70% of the included patients received neoadjuvant therapy of nanoparticle albumin-bound-paclitaxel/platinum (cisplatin or carboplatin) plus PD-1 inhibitor, while the remaining ones received platinum (cisplatin or carboplatin)/5-Fluorouracil (5-FU) plus PD-1 inhibitor. The pCR probability was 48.3% for all patients, which were 43.2–51.0% for the training and validation sets. None of the characteristics were significantly different among the training and validation sets (p>0.05).

Feature selection and radiomics signature construction

In total, 1,304×2 sequences (T1+C, T2WI)×8 segments (1 tumor+7 peritumoral)=20,864 features were exacted out from MR image for each patient. After the stability test, 20,024 features were retained with ICC>0.75. The features extracted from each segment were processed to filter redundant and non-predictive features using the LASSO algorithm, respectively. The screened-out features from different segments are shown in table 2. Radiomics scores of intratumoral and each peritumoral areas were calculated (online supplemental table 2). There was a significant difference of Rad-scores (all p<0.05) between pCR subgroup and non-pCR subgroup. The Rad-score of either tumoral area or each peritumoral area could clarify pCR and non-pCR subgroup effectively. The ability of the Rad-score of −3 to 0 mm peritumoral area outperformed other peritumoral Rad-scores in predicting pCR in the training cohort, which was identified as the best peritumoral Rad-score (peri-Rad-score) (online supplemental figure 3).

Construction and validation of the radiomics-clinical nomogram

Rad-scores and clinicopathological characteristics were included in the univariate and multivariate logistic regression analysis. Intratumoral Rad-score (intra-Rad-score), peritumoral Rad-score of −3 to 0 mm (peri-Rad-score), and CPS were identified as independent predictors of pCR in patients with HNSCC, which a radiomics-clinical nomogram (radiomics-clinical nomogram II) was developed based on (table 3 and figure 2A). For the diagnosis of collinearity, the VIF of the 16 predictors ranged from 1.098 to 2.919, indicating the absence of collinearity. The ROC analysis showed that radiomics-clinical nomogram II achieved an AUC of 0.904 (95% CI, 0.835 to 0.972) in the training cohort, 0.860 (95% CI, 0.722 to 0.998) in the internal validation cohort, and 0.849 (95% CI, 0.739 to 0.959) in the external validation cohort (figure 2B–D). The sensitivities and specificities spanned from 73.1% to 87.8% and from 86.0% to 96.0% in training and validation sets, respectively (details shown in online supplemental table 3). The calibration curve showed good calibration (figure 2E–G).

Clinical utility assessment of the radiomics-clinical nomogram

Another radiomics-clinical nomogram (radiomics-clinical nomogram I) was developed based on intra-Rad-score and clinicopathological characteristics, which incorporated intra-Rad-score, CPS and chemotherapy regimens (figure 3A and online supplemental table 4). A clinical one (clinical nomogram) was based on clinical independent predictors, CPS and chemotherapy regimens (figure 3B and online supplemental table 5). The AUC of radiomics-clinical nomogram II was significantly higher than those of radiomics-clinical nomogram I, clinical nomogram, Rad-scores, and CPS (all p<0.001, figure 3C, online supplemental table 6). 89 patients were predicted to achieve pCR using radiomics-clinical nomogram II in all included 172 patients, of which 69 (77.5%) patients achieved pCR in pathologic examination and 78 (87.6%) ones achieved major pathologic response (MPR) among. pCR ratio and MPR ratio in the subgroup predicted to achieve pCR using radiomics-clinical nomogram II was higher than that using CPS (69.7% and 84.2%, respectively), a widely employed biomarker in HNSCC.

Table 1 Patients' clinicopathological characteristics

Variable	Patients (n=172)	Training set (n=84)	Internal test set (n=37)	External test set (n=51)	P value
Age*/years	54.6±11.9	56.0±11.4	53.5±12.5	53.1±12.3	0.320
Gender/n, %					0.504
Female	39 (22.7)	17 (20.2)	11 (29.7)	11 (21.6)	
Male	133 (77.3)	67 (79.8)	26 (70.3)	40 (78.4)	
Primary tumor site/n, %					0.541
Oral cavity	90 (52.3)	41 (48.8)	20 (54.1)	29 (56.9)	
Oropharynx	51 (29.7)	24 (28.6)	10 (27.0)	17 (33.3)	
Hypopharynx	17 (9.9)	12 (14.3)	3 (8.1)	2 (3.9)	
Larynx	14 (8.1)	7 (8.3)	4 (10.8)	3 (5.9)	
T status/n, %					0.908
T1	2 (1.2)	1 (1.2)	1 (2.7)	0	
T2	60 (34.9)	27 (32.1)	13 (35.1)	20 (39.2)	
T3	65 (37.8)	33 (39.3)	13 (35.1)	19 (37.3)	
T4a	45 (26.2)	23 (27.4)	10 (27.0)	12 (23.5)	
N status/n, %					0.289
N0	80 (46.5)	39 (46.4)	23 (62.2)	18 (35.3)	
N1	11 (6.4)	5 (6.0)	1 (2.7)	5 (9.8)	
N2b	57 (33.1)	27 (32.1)	9 (24.3)	21 (41.2)	
N2c	24 (14.0)	13 (15.5)	4 (10.8)	7 (13.7)	
Prognostic stage/n, %					0.968
II	44 (25.6)	22 (26.2)	10 (27.0)	12 (23.5)	
III	47 (27.3)	23 (27.4)	11 (29.7)	13 (25.5)	
IV	81 (47.1)	39 (46.4)	16 (43.2)	26 (51.0)	
Histologic grade/n, %					0.758
Grade I	51 (29.7)	25 (29.8)	12 (32.4)	14 (27.5)	
Grade II	100 (58.1)	47 (56.0)	20 (54.1)	33 (64.7)	
Grade III	21 (12.2)	12 (14.3)	5 (13.5)	4 (7.8)	
Grade IV	0	0	0		
p16/n,%					0.889
Negative	112 (65.1)	56 (66.7)	23 (62.2)	33 (64.7)	
Positive	60 (34.9)	28 (33.3)	14 (37.8)	18 (35.3)	
Combined positive score/median, range	30 (1–100)	30 (1–95)	25 (1–00)	30 (1–90)	0.172
Tobacco consumption/n, %					0.149
No	32 (18.6)	13 (15.5)	5 (13.5)	14 (27.5)	
Yes	140 (81.4)	71 (84.5)	32 (86.5)	37 (72.5)	
Alcohol consumption/n, %					0.913
No	69 (40.1)	35 (41.7)	14 (37.8)	20 (39.2)	
Yes	103 (59.9)	49 (58.3)	23 (62.2)	31 (60.8)	
Neoadjuvant therapy regimen/n, %					0.256
nab-PP+anti-PD-1	127 (73.8)	59 (70.2)	26 (70.3)	42 (82.4)	
PF+anti-PD-1	45 (26.2)	25 (29.8)	11 (29.7)	9 (17.6)	

Continued

Table 1 Continued

Variable	Patients (n=172)	Training set (n=84)	Internal test set (n=37)	External test set (n=51)	P value
Immunotherapy drug					0.457
Tislelizumab	69 (40.1)	33 (39.3)	16 (43.2)	20 (39.2)	
Pembrolizumab	70 (40.7)	39 (46.4)	13 (35.1)	18 (35.3)	
Nivolumab	19 (11.0)	7 (8.3)	6 (16.2)	6 (11.8)	
Sintilizumab	14 (8.1)	5 (6.0)	2 (5.4)	7 (13.7)	
Neoadjuvant therapy cycles/n, %					0.225
2	75 (43.6)	42 (50.0)	14 (37.8)	19 (37.3)	
3	97 (56.4)	42 (50.0)	23 (62.2)	32 (62.7)	
Treatment response					0.766
pCR	83 (48.3%)	41 (48.8%)	16 (43.2%)	26 (51.0%)	
Non-pCR	89 (51.7%)	43 (51.2%)	21 (56.8%)	25 (49.0%)	

*The variable is summarized as mean and SD (mean±SD).
nab-PP, nanoparticle albumin-bound-paclitaxel/platinum (cisplatin or carboplatin); pCR, pathologic complete response; PD-1, programmed death receptor-1; PF, platinum (cisplatin or carboplatin)/5-Fluorouracil (5-FU).

The DCA curve for radiomics-clinical nomogram II showed that the radiomic-clinical nomogram adds more net benefit than the "treat all" or "treat none" strategies at all given threshold probability (figure 3D).

The performance of radiomics-clinical nomogram II in oral and oropharyngeal SCC

The performance of radiomics-clinical nomogram II was tested in the subgroups of the patients with oral and oropharyngeal SCC, respectively. Radiomics-clinical nomogram II achieved high accuracy in discriminating pCR and non-pCR response status with AUC of 0.816 (95% CI, 0.725 to 0.906) in oral SCC and 0.928 (95% CI, 0.860 to 0.996) in oropharyngeal SCC, respectively, which were superior to radiomics-clinical nomogram I, clinical nomogram, peri-Rad-score, intra-Rad-score and CPS (figure 4A–B).

Correlation between radiomics features and pathologic characteristics

Biopsy samples of 38 patients obtained before neoadjuvant therapy were included in the correlation analysis of radiomics features and pathologic characteristics. The results revealed that some of intratumoral and peritumoral radiomics features were associated with immune cell density, fibroblast density and immune cell ratios

Table 2 The screened-out features and coefficient from different segments

ROI	Feature	Coefficient
Intratumoral ROI	t1_wavelet.LLH_firstorder_10Percentile	0.0022
	t1_wavelet.LLH_firstorder_Minimum	0.0009
	t1_wavelet.HLH_glrlm_GrayLevelVariance	–0.0017
Peritumoral ROI I	t1_log.sigma.5.0.mm.3D_glszm_SmallAreaLowGrayLevelEmphasis	–0.7585
	t2_wavelet.LHL_glszm_SmallAreaEmphasis	1.8728
	t2_wavelet.LHH_firstorder_Median	356.5238
	t2_wavelet.HLH_glrlm_RunVariance	–0.5999
Peritumoral ROI II	t1_wavelet.LLL_glszm_SmallAreaEmphasis	–1.0257
	t2_wavelet.LLH_glrlm_LongRunLowGrayLevelEmphasis	–0.0028
Peritumoral ROI III	t2_wavelet.LLH_gldm_LargeDependenceLowGrayLevelEmphasis	–0.0062
	t2_wavelet.LLH_glrlm_ShortRunLowGrayLevelEmphasis	4.3114
	t2_wavelet.HLH_glrlm_LongRunLowGrayLevelEmphasis	–0.0043
	t2_squareroot_firstorder_Maximum	0.0068

Peritumoral ROI I refers to the peritumoral area with inward 3 mm. Peritumoral ROI II refers to the peritumoral area with inward 3 mm and outward 3 mm. Peritumoral ROI III refers to the peritumoral area with inward 3 mm and outward 6 mm.
ROI, region of interest.

Table 3 Univariate and multivariate logistic regression analysis of clinicopathological characteristics and Rad-scores in the training set

	Univariate logistic regression		Multivariate logistic regression	
Variable	**OR (95% CI)**	**P value**	**OR (95% CI)**	**P value**
Age	1.008 (0.971, 1.047)	0.664		
Gender	0.359 (0.114, 1.131)	0.080		
Primary tumor site		0.627		
Oral cavity	Reference			
Oropharynx	0.980 (0.357, 2.692)	0.968		
Hypopharynx	2.316 (0.601, 8.916)	0.222		
Larynx	0.868 (0.172, 4.379)	0.864		
T status		0.722		
T1	2512960866.657 (-)	1		
T2	1.944 (0.628, 6.021)	0.249		
T3	1.464 (0.497, 4.313)	0.489		
T4a	Reference			
N status		0.15		
N0	Reference			
N1	6.400 (0.652, 62.840)	0.111		
N2b	1.486 (0.550, 4.010)	0.435		
N2c	3.600 (0.940, 13.788)	0.062		
Prognostic stage group		0.665		
II	Reference			
III	0.909 (0.282, 2.935)	0.873		
IV	0.644 (0.225, 1.842)	0.412		
Histologic grade		0.659		
Grade I	Reference			
Grade II	1.446 (0.545, 3.387)	0.459		
Grade III	0.909 (0.226, 3.661)	0.893		
p16	1.653 (0.662, 4.129)	0.282		
Combined positive score	1.028 (1.010, 1.045)	0.002	1.048 (1.019, 1.077)	0.001
Tobacco consumption	1.134 (0.347, 3.712)	0.835		
Alcohol consumption	0.686 (0.287, 1.640)	0.397		
Chemotherapy regimen	4.025 (1.455, 11.137)	0.007		
Immunotherapy drug		0.36		
Tislelizumab	Reference			
Pembrolizumab	1.240 (0.490, 3.138)	0.65		
Nivolumab	0.177 (0.019, 1.638)	0.127		
Sintilizumab	1.594 (0.235, 10.817)	0.633		
Neoadjuvant therapy cycles	1.100 (0.467, 2.589)	0.827		
Intra-Rad-score	195.213 (9.952, 3829.289)	0.001	62.970 (1.059, 3743.196)	0.047
Peri-Rad-score	112.525 (13.295, 952.397)	<0.001	118.169 (8.369, 1668.637)	<0.001

Intra-Rad-score refers to the radiomics score of intratumoral area. Peri-Rad-score refers to the radiomics score of the peritumoral area with inward 3 mm.
pCR, pathologic complete response.

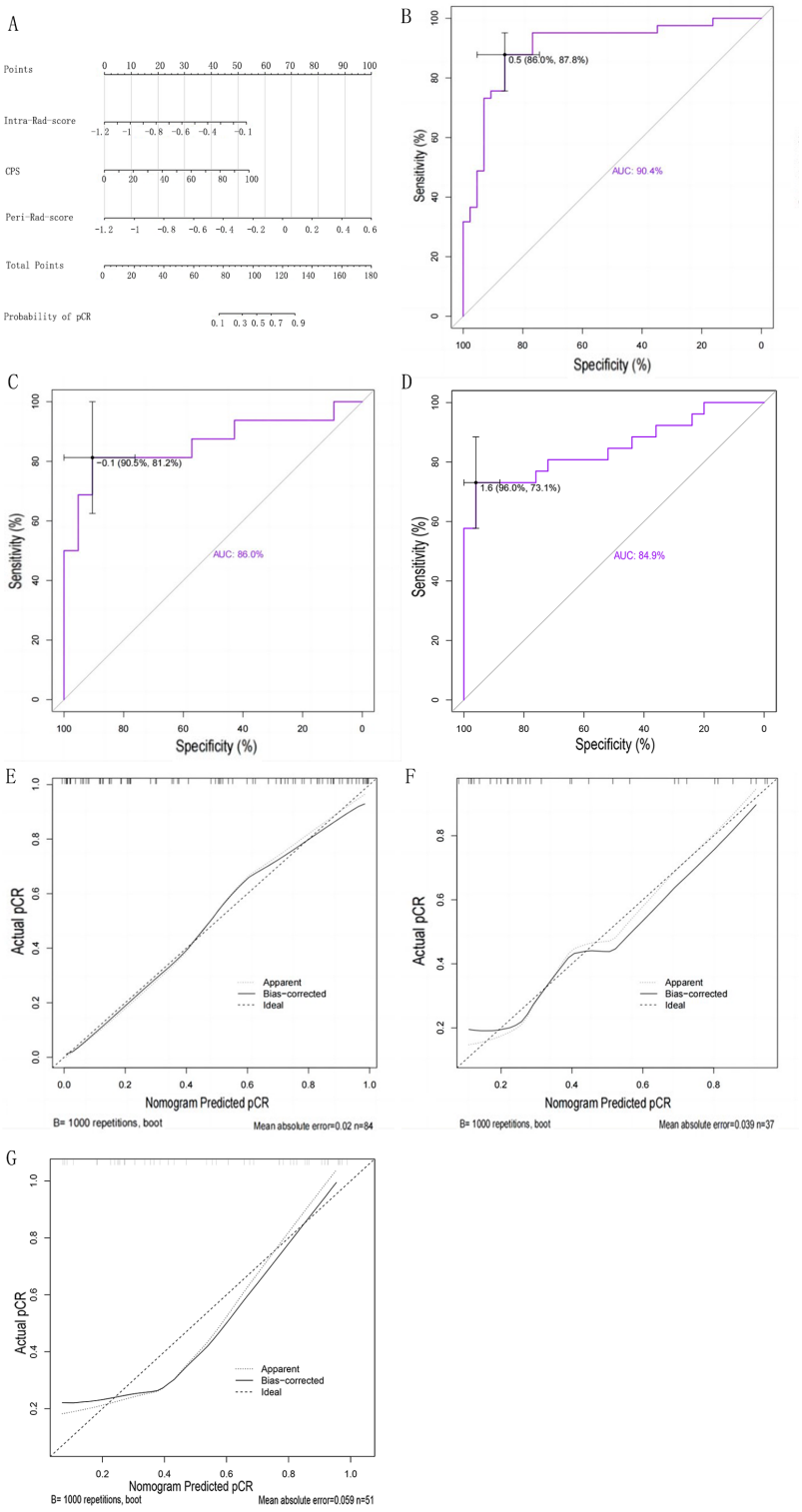

Figure 2 Construction and validation of the radiomics-clinical nomogram performance. (A) Radiomics-clinical nomogram for the prediction of pathologic complete response to neoadjuvant chemoimmunotherapy in head and neck squamous cell carcinoma. (B) Receiver operator characteristic curves of the radiomics-clinical nomogram in the training set. (C) Receiver operator characteristic curves of the radiomics-clinical nomogram in the internal validation set. (D) Receiver operator characteristic curves of the radiomics-clinical nomogram in the external validation set. (E) Calibration curves of the radiomics-clinical nomogram in the training set. (F) Calibration curves of the radiomics-clinical nomogram in the internal validation set. (G) Calibration curves of the radiomics-clinical nomogram in the external validation set. Calibration curves depict agreement between the nomogram-predicted probability of pCR (x-axis) and the actual probability of pCR (y-axis). Dashed line=ideal nomogram; dotted line=apparent predicted accuracy; solid line=calibration estimate from the internally validated model. Perfect prediction would correspond to the dashed line. AUC, area under the receiver operator characteristic curve; CPS, combined positive score; pCR, pathologic complete response.

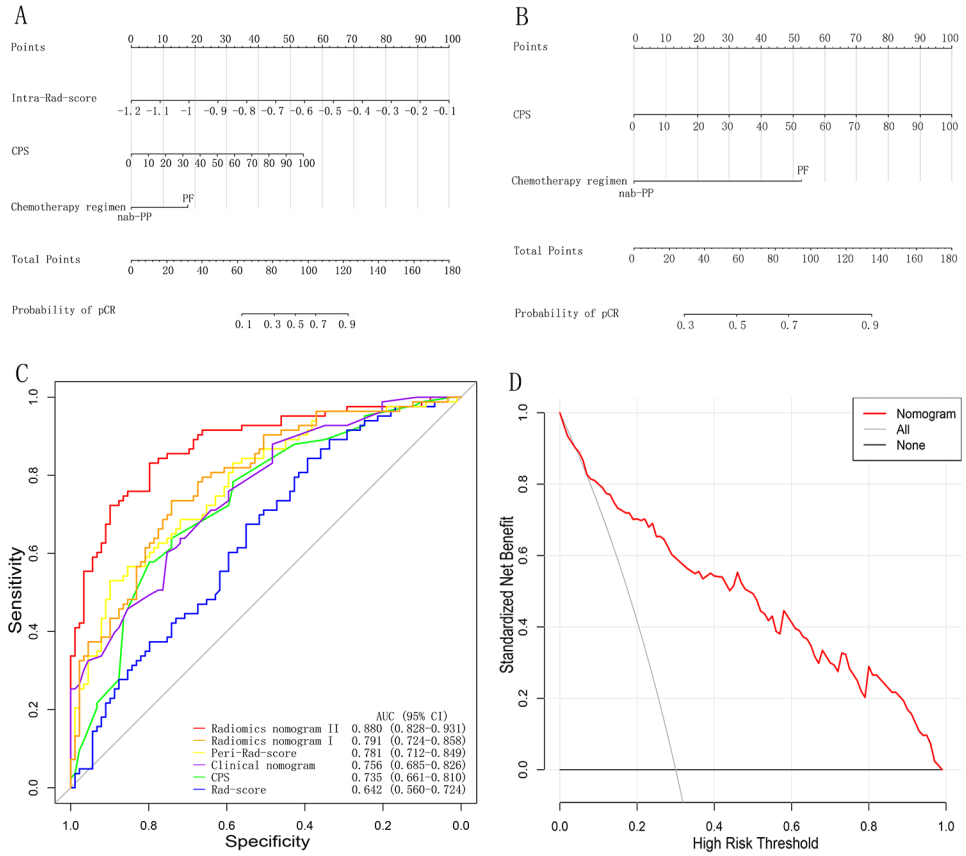

Figure 3 Clinical utility assessment of the radiomics-clinical nomogram. (A) Radiomics-clinical nomogram developed based on intratumoral radiomics features and clinicopathological characteristics. (B) Radiomics-clinical nomogram developed based on clinicopathological characteristics. (C) Receiver operator characteristic curves of the nomograms, CPS, Rad-scores in all 172 patients. Radiomics-clinical nomogram I refers to the radiomics-clinical nomogram based on intratumoral radiomics score and clinicopathological characteristics. Radiomics-clinical nomogram II refers to the radiomics-clinical nomogram based on intratumoral radiomics score, peritumoral radiomics score and clinicopathological characteristics. Intra-Rad-score refers to the radiomics score of intratumoral area. Peri-Rad-score refers to the radiomics score of the peritumoral area with inward 3 mm. (D) DCA for the nomogram. The net benefit was plotted versus the threshold probability, the value of the lowest suspected probability of pCR to advise the patient to receive neoadjuvant chemoimmunotherapy. The red line represents the radiomics-clinical nomogram. The gray and black lines represent the hypothesis that all patients and no patients received neoadjuvant chemoimmunotherapy. AUC, area under the receiver operator characteristic curve; CPS, combined positive score; DCA, decision curve analysis; pCR, pathologic complete response.

(detail shown in online supplemental table 7). Intra-Rad-score demonstrated associations with immune cell density, fibroblast density, etTILs%, eTILs%, and esTILs% within the intratumoral region. Meanwhile, peri-Rad-score was linked to overall cell density, immune cell density, etTILs%, and eTILs% in the peritumoral zone. These correlation analyses suggested that radiomic features from both intratumoral and peritumoral areas might be capable of reflecting TILs and fibroblast information, which could be instrumental in predicting responses to NACI in HNSCC.

DISCUSSION

In recent years, administration of immune checkpoint inhibitors seemed to be a promising approach in the treatment of HNSCC, especially after the results from KEYNOTE-048 and KEYNOTE-040 trials were reported. The KEYNOTE-048 trial compared treatment with pembrolizumab, an anti-PD-1 antibody, with or without chemotherapy, versus the EXTREME regimen for R/M HNSCCs, and drew a conclusion that pembrolizumab with chemotherapy improved OS in the total population and pembrolizumab alone improved OS in the population with CPS of 1 or more. The results from KEYNOTE-040 trial showed that pembrolizumab alone improved OS compared with the standard of care for the patients with R/M HNSCC that progressed during or after platinum-containing treatment, or the patients with locally advanced HNSCC that recurred or progressed within 3–6 months after platinum-containing treatment.[5 25] These inspiring results supported pembrolizumab as a first-line treatment for R/M HNSCCs.[6]

In consideration of the better immune status, fewer drug-resistant clones and less genetic heterogeneity, neoadjuvant immunotherapy may induce more robust expansion of tumor-specific T cells before local treatment

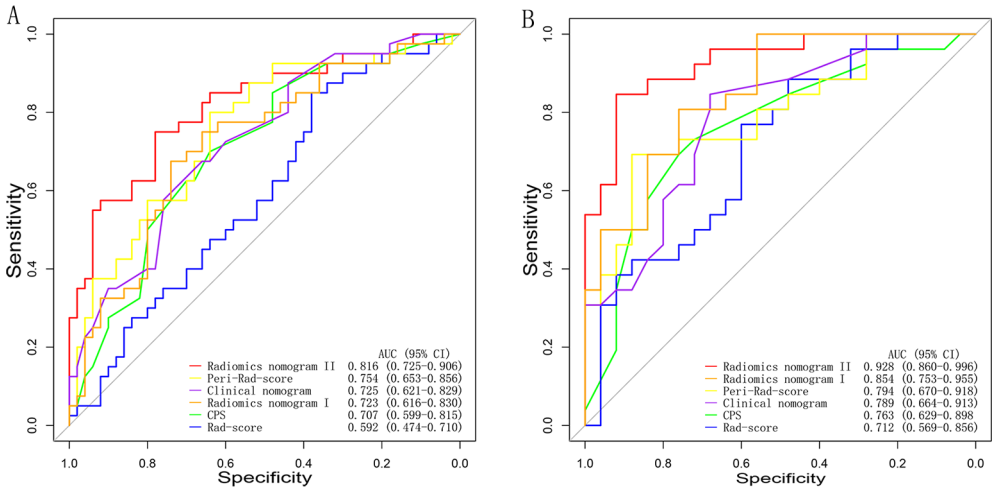

Figure 4 Receiver operator characteristic curves of the nomograms, CPS, Rad-scores in oral SCC (A) and oropharyngeal SCC (B). Radiomics-clinical nomogram I refers to the radiomics-clinical nomogram based on intratumoral radiomics score and clinicopathological characteristics. Radiomics-clinical nomogram II refers to the radiomics-clinical nomogram based on intratumoral radiomics score, peritumoral radiomics score and clinicopathological characteristics. Intra-Rad-score refers to the radiomics score of intratumoral area. Peri-Rad-score refers to the radiomics score of the peritumoral area with inward 3 mm. AUC, area under the receiver operator characteristic curve; CPS, combined positive score; SCC, squamous cell carcinoma.

and achieve more inspiring results than that for R/M HNSCC.[26] However, response to neoadjuvant immunomonotherapy or dual-drug immunotherapy varied for newly diagnosed HNSCCs in published studies, with pCR from 0.0% to 6.7% and MPR from 5.9% to 35.0%.[8 27–29] Based on the experience of the combination of chemotherapy and pembrolizumab in the KEYNOTE-048 study and the studies for other malignancies, chemotherapy was considered to enhance antitumor immunity through inducing tumor cell death, promoting tumor neoantigen release and modifying tumor microenvironment (TME).[30] Several studies confirmed that pCR rates from neoadjuvant chemoimmunotherapy were obviously higher than those from neoadjuvant immunotherapy, which increased from 36.4% to 42.0% in the neoadjuvant chemoimmunotherapy cohorts.[9 28 29 31 32] On account of the nearly 40% of pCR, which was proved to indicate better prognosis in several studies, neoadjuvant chemoimmunotherapy has fueled increasing interest in the possibility of treatment de-escalation and function preservation for locally advanced HNSCC.[10–12] However, it is difficult to predict and assess pathological responses, especially pCR, to neoadjuvant chemoimmunotherapy with high accuracy using non-invasive procedures for now. The patients with less responsiveness to neoadjuvant chemoimmunotherapy may suffer from the complications caused by neoadjuvant chemoimmunotherapy, even delay of radical surgery or concurrent chemoradiotherapy without prognosis improvement.[14] Therefore, it is significant to develop a non-invasive procedure to predict or assess pathological response to neoadjuvant chemoimmunotherapy with high accuracy for HNSCC.

Current approaches to predict response to immunotherapy for HNSCC and other cancers mainly rely on biomarkers such as programmed death ligand 1 expression (CPS), tumor mutation burden, and microsatellite instability. CPS is the most widespread-used biomarker in clinical practice. However, whether these biomarkers can predict responses from the combined chemoimmunotherapy remains unclear.[16] Furthermore, these biomarkers could not adequately characterize the spatial heterogeneity of tumors. Radiomics is an explicitly designed process, which could extract innumerable quantitative features from digital medical images.[18 33] It seems that radiomics has great potential to assist in disease detection, diagnosis, treatment response and prognosis prediction through supplying nearly limitless image biomarkers.[18 34–37] In this study, we employed a high-throughput radiomics method to developed and validated an MRI-based radiomics-clinical nomogram to predict pCR to neoadjuvant chemoimmunotherapy for HNSCC. This radiomics-clinical nomogram yielded a great performance in the prediction of pCR with AUC of 0.904, 0.860 and 0.849 in the training, the internal validation and the external validation sets, respectively. The predicting accuracy of the radiomics-clinical nomogram outperformed those of CPS, clinical nomogram and Rad-scores alone (all $p<0.001$).

TME plays a crucial role in the progression of malignancies and influences response to immunotherapy for different types of cancers.[38–40] Peritumoral and intratumoral areas may have a different composition of cell types and be valued differently in immunotherapy.[38 41] Some researchers tried to classify TME based on different density of immune cells within intratumoral and peritumoral area, which was shown to be associated with response to immunotherapy and prognosis of various types of cancers.[38 41 42] Some latest studies revealed that there may be an intrinsic relationship between radiomics features and TME.[43–45] Braman *et al* reported a

significant correlation between peritumoral radiomic features and lymphocytic density.[43] Hu *et al* demonstrated that the radiomics model might be related to lymphocyte-mediated immunity and cytokines such as interferons and interleukins.[44] The radiomics features, which were related to TME, may turn out to be valuable biomarkers in assistance of cancer detection, diagnosis, treatment response prediction, *et al*. In our study, we extracted features from different peritumoral areas and found out the area from −3 to 0 mm played the most important role in predicting treatment response to neoadjuvant chemoimmunotherapy. Whole-slide tissue analysis indicated that the ratios of immune cells (etTIL% and esTIL%) were significantly elevated in the peritumoral zone as compared with the intratumoral region (online supplemental table 8). Radiomic features correlated with immune cells density, fibroblasts density, and immune cell ratios in both peritumoral and intratumoral areas. The nomogram incorporating peritumoral and intratumoral Rad-scores simultaneously achieved a better predicting accuracy with an AUC of 0.880 (95% CI, 0.828 to 0.931), which was significantly higher than that of the nomogram developed only based on intratumoral radiomics features and clinicopathological characteristics in the combined training and validation set ($p<0.001$, figure 3C and online supplemental table 6). These results indicated that peritumoral radiomics features could provide incremental value in predicting responses to neoadjuvant chemoimmunotherapy for HNSCC.

Still, this study had several limitations. First, it had a limited sample size due to the relatively low incidence of HNSCC compared with some other malignancies. Second, the retrospective nature of the study may introduce some potential bias. The results would be needed to be validated in prospective studies with a larger sample size in the future.

In conclusion, peritumoral and intratumoral radiomics features could provide valuable information in predicting response to neoadjuvant chemoimmunotherapy with traditional chemotherapy plus an anti-PD-1 antibody for HNSCC, and the radiomics-clinical nomogram is a useful non-invasive tool in predicting pCR for these patients.

Author affiliations
[1]Guangdong Provincial Key Laboratory of Malignant Tumor Epigenetics and Gene Regulation, Sun Yat-Sen Memorial Hospital, Guangzhou, Guangdong, China
[2]Department of Otolaryngology, Sun Yat-Sen Memorial Hospital, Guangzhou, Guangdong, China
[3]Department of Radiology, Sun Yat-Sen Memorial Hospital, Guangzhou, Guangdong, China
[4]Pathology Department, Sun Yat-Sen Memorial Hospital, Guangzhou, Guangdong, China
[5]Cellular & Molecular Diagnostics Center, Sun Yat-Sen Memorial Hospital, Guangzhou, Guangdong, China
[6]Department of Otolaryngology, Shenshan Medical Centre, Memorial Hospital of Sun Yat-sen University, Shanwei, China
[7]Department of Head and Neck Surgery, Sun Yat-sen University Cancer Center, Guangzhou, Guangdong, China
[8]Department of Oral and Maxillofacial Surgery, Sun Yat-Sen Memorial Hospital, Guangzhou, Guangdong, China

Contributors Study design: PL, WX, YL, XL, SF, and XH. Data collection: WX, YL, CZ, FL, GC, and SF. Data analysis: PL, WX, YL, CZ, HWu, HWa, MG, GC, SF, and XH. Writing original draft: PL, WX, and YL. Literature search: PL, WX, YL, GC, SF, and XH. Resources: PL, YL, HWu, FL, GC, SF, and XH. Funding acquisition: PL. Supervision: PL, XL, SF, and XH. Review and editing: All authors. XH is responsible for the overall content as guarantor.

Funding This study was supported by the National Natural Science Foundation of China (No. 82101238) and Guangzhou Municipal Science and Technology Project (No. 2024A03J1187 and No. 202201011316). The funding sponsors were not involved in study design, data collection, analysis, interpretation, or any aspect pertinent to the study.

Competing interests No, there are no competing interests.

Patient consent for publication Not applicable.

Provenance and peer review Not commissioned; externally peer reviewed.

Data availability statement Data are available in a public, open access repository. The data underlying this article are available in Mendeley Data, V2, doi: 10.17632/c26vbcxhcx.2.

ORCID iDs
Peiliang Lin http://orcid.org/0000-0002-9859-8199
Ping Han http://orcid.org/0000-0001-6097-7794
Xiaoming Huang http://orcid.org/0000-0002-5859-533X

REFERENCES

1 Marur S, Forastiere AA. Head and Neck Squamous Cell Carcinoma: Update on Epidemiology, Diagnosis, and Treatment. *Mayo Clin Proc* 2016;91:386–96.
2 Bray F, Ferlay J, Soerjomataram I, *et al*. Global cancer statistics 2018: GLOBOCAN estimates of incidence and mortality worldwide for 36 cancers in 185 countries. *CA Cancer J Clin* 2018;68:394–424.
3 Siegel RL, Miller KD, Fuchs HE, *et al*. Cancer statistics, 2022. *CA Cancer J Clin* 2022;72:7–33.
4 Siegel RL, Miller KD, Jemal A. Cancer statistics, 2016. *CA A Cancer J Clinicians* 2016;66:7–30.
5 Burtness B, Harrington KJ, Greil R, *et al*. Pembrolizumab alone or with chemotherapy versus cetuximab with chemotherapy for recurrent or metastatic squamous cell carcinoma of the head and neck (KEYNOTE-048): a randomised, open-label, phase 3 study. *Lancet* 2019;394:1915–28.
6 National Comprehensive Cancer Network. Version 1. (NCCN) clinical practice guidelines in oncology. *Head and Neck Cancers, Version 1*; 2024.
7 Cabezas-Camarero S, Alonso-Ovies A, Merino-Menéndez S, *et al*. Major pathological response and durable locoregional control after neoadjuvant pembrolizumab-carboplatin-paclitaxel in head and neck cancer. *Oral Oncol* 2021;123:105589.
8 Vos JL, Elbers JBW, Krijgsman O, *et al*. Neoadjuvant immunotherapy with nivolumab and ipilimumab induces major pathological responses in patients with head and neck squamous cell carcinoma. *Nat Commun* 2021;12:7348.
9 Zhang Z, Wu B, Peng G, *et al*. Neoadjuvant Chemoimmunotherapy for the Treatment of Locally Advanced Head and Neck Squamous

Cell Carcinoma: A Single-Arm Phase 2 Clinical Trial. *Clin Cancer Res* 2022;28:3268–76.
10 Maas M, Nelemans PJ, Valentini V, *et al*. Long-term outcome in patients with a pathological complete response after chemoradiation for rectal cancer: a pooled analysis of individual patient data. *Lancet Oncol* 2010;11:835–44.
11 He J, Blair AB, Groot VP, *et al*. Is a Pathological Complete Response Following Neoadjuvant Chemoradiation Associated With Prolonged Survival in Patients With Pancreatic Cancer? *Ann Surg* 2018;268:1–8.
12 Spring LM, Fell G, Arfe A, *et al*. Pathologic Complete Response after Neoadjuvant Chemotherapy and Impact on Breast Cancer Recurrence and Survival: A Comprehensive Meta-analysis. *Clin Cancer Res* 2020;26:2838–48.
13 Zhong L, Zhang C, Ren G, *et al*. Randomized phase III trial of induction chemotherapy with docetaxel, cisplatin, and fluorouracil followed by surgery versus up-front surgery in locally advanced resectable oral squamous cell carcinoma. *J Clin Oncol* 2013;31:744–51.
14 Tang AL, O'Neil T, McDermott S, *et al*. Association of Neoadjuvant Pembrolizumab for Oral Cavity Squamous Cell Carcinoma With Adverse Events After Surgery in Treatment-Naive Patients. *JAMA Otolaryngol Head Neck Surg* 2022;148:935.
15 Luchini C, Bibeau F, Ligtenberg MJL, *et al*. ESMO recommendations on microsatellite instability testing for immunotherapy in cancer, and its relationship with PD-1/PD-L1 expression and tumour mutational burden: a systematic review-based approach. *Ann Oncol* 2019;30:1232–43.
16 Cheng A-L, Hsu C, Chan SL, *et al*. Challenges of combination therapy with immune checkpoint inhibitors for hepatocellular carcinoma. *J Hepatol* 2020;72:307–19.
17 Lambin P, Leijenaar RTH, Deist TM, *et al*. Radiomics: the bridge between medical imaging and personalized medicine. *Nat Rev Clin Oncol* 2017;14:749–62.
18 Gillies RJ, Kinahan PE, Hricak H. Radiomics: Images Are More than Pictures, They Are Data. *Radiology* 2016;278:563–77.
19 Xu B, Dong S-Y, Bai X-L, *et al*. Tumor Radiomic Features on Pretreatment MRI to Predict Response to Lenvatinib plus an Anti-PD-1 Antibody in Advanced Hepatocellular Carcinoma: A Multicenter Study. *Liver Cancer* 2023;12:262–76.
20 Liu Z, Zhang X-Y, Shi Y-J, *et al*. Radiomics Analysis for Evaluation of Pathological Complete Response to Neoadjuvant Chemoradiotherapy in Locally Advanced Rectal Cancer. *Clin Cancer Res* 2017;23:7253–62.
21 Liu C, Zhao W, Xie J, *et al*. Development and validation of a radiomics-based nomogram for predicting a major pathological response to neoadjuvant immunochemotherapy for patients with potentially resectable non-small cell lung cancer. *Front Immunol* 2023;14:1115291.
22 Ma J, Chen K, Li S, *et al*. MRI-based radiomic models to predict surgical margin status and infer tumor immune microenvironment in breast cancer patients with breast-conserving surgery: a multicenter validation study. *Eur Radiol* 2024;34:1774–89.
23 van Griethuysen JJM, Fedorov A, Parmar C, *et al*. Computational Radiomics System to Decode the Radiographic Phenotype. *Cancer Res* 2017;77:e104–7.
24 Xirou V, Moutafi M, Bai Y, *et al*. An algorithm for standardization of tumor Infiltrating lymphocyte evaluation in head and neck cancers. *Oral Oncol* 2024;152:106750.
25 Cohen EEW, Soulières D, Le Tourneau C, *et al*. Pembrolizumab versus methotrexate, docetaxel, or cetuximab for recurrent or metastatic head-and-neck squamous cell carcinoma (KEYNOTE-040): a randomised, open-label, phase 3 study. *The Lancet* 2019;393:156–67.
26 Ferrarotto R, Bell D, Rubin ML, *et al*. Impact of Neoadjuvant Durvalumab with or without Tremelimumab on CD8$^+$ Tumor Lymphocyte Density, Safety, and Efficacy in Patients with Oropharynx Cancer: CIAO Trial Results. *Clin Cancer Res* 2020;26:3211–9.
27 Knochelmann HM, Horton JD, Liu S, *et al*. Neoadjuvant presurgical PD-1 inhibition in oral cavity squamous cell carcinoma. *Cell Rep Med* 2021;2:100426.
28 Ferris RL, Spanos WC, Leidner R, *et al*. Neoadjuvant nivolumab for patients with resectable HPV-positive and HPV-negative squamous cell carcinomas of the head and neck in the CheckMate 358 trial. *J Immunother Cancer* 2021;9:e002568.
29 Schoenfeld JD, Hanna GJ, Jo VY, *et al*. Neoadjuvant Nivolumab or Nivolumab Plus Ipilimumab in Untreated Oral Cavity Squamous Cell Carcinoma: A Phase 2 Open-Label Randomized Clinical Trial. *JAMA Oncol* 2020;6:1563–70.
30 Judd J, Borghaei H. Combining Immunotherapy and Chemotherapy for Non-Small Cell Lung Cancer. *Thorac Surg Clin* 2020;30:199–206.
31 Uppaluri R, Campbell KM, Egloff AM, *et al*. Neoadjuvant and Adjuvant Pembrolizumab in Resectable Locally Advanced, Human Papillomavirus-Unrelated Head and Neck Cancer: A Multicenter, Phase II Trial. *Clin Cancer Res* 2020;26:5140–52.
32 Wang K, Gui L, Lu H, *et al*. Efficacy and safety of pembrolizumab with preoperative neoadjuvant chemotherapy in patients with resectable locally advanced head and neck squamous cell carcinomas. *Front Immunol* 2023;14:1189752.
33 Lambin P, Rios-Velazquez E, Leijenaar R, *et al*. Radiomics: Extracting more information from medical images using advanced feature analysis. *Eur J Cancer* 2012;48:441–6.
34 Lu S, Ling H, Chen J, *et al*. MRI-based radiomics analysis for preoperative evaluation of lymph node metastasis in hypopharyngeal squamous cell carcinoma. *Front Oncol* 2022;12.
35 Wang F, Tan R, Feng K, *et al*. Magnetic Resonance Imaging-Based Radiomics Features Associated with Depth of Invasion Predicted Lymph Node Metastasis and Prognosis in Tongue Cancer. *Magnetic Resonance Imaging* 2022;56:196–209.
36 Chen J, Lu S, Mao Y, *et al*. An MRI-based radiomics-clinical nomogram for the overall survival prediction in patients with hypopharyngeal squamous cell carcinoma: a multi-cohort study. *Eur Radiol* 2022;32:1548–57.
37 Corti A, De Cecco L, Cavalieri S, *et al*. MRI-based radiomic prognostic signature for locally advanced oral cavity squamous cell carcinoma: development, testing and comparison with genomic prognostic signatures. *Biomark Res* 2023;11:69.
38 Adegoke NA, Gide TN, Mao Y, *et al*. Classification of the tumor immune microenvironment and associations with outcomes in patients with metastatic melanoma treated with immunotherapies. *J Immunother Cancer* 2023;11:e007144.
39 Li Y, Wang P, Xu J, *et al*. Noninvasive radiomic biomarkers for predicting pseudoprogression and hyperprogression in patients with non-small cell lung cancer treated with immune checkpoint inhibition. *Oncoimmunology* 2024;13:2312628.
40 Knebel M, Körner S, Kühn JP, *et al*. Prognostic impact of intra- and peritumoral immune cell subpopulations in head and neck squamous cell carcinomas - comprehensive analysis of the TCGA-HNSC cohort and immunohistochemical validation on 101 patients. *Front Immunol* 2023;14:1172768.
41 Galon J, Bruni D. Approaches to treat immune hot, altered and cold tumours with combination immunotherapies. *Nat Rev Drug Discov* 2019;18:197–218.
42 Gruosso T, Gigoux M, Manem VSK, *et al*. Spatially distinct tumor immune microenvironments stratify triple-negative breast cancers. *J Clin Invest* 2019;129:96313:1785–800:.
43 Braman N, Prasanna P, Whitney J, *et al*. Association of Peritumoral Radiomics With Tumor Biology and Pathologic Response to Preoperative Targeted Therapy for HER2 (ERBB2)-Positive Breast Cancer. *JAMA Netw Open* 2019;2:e192561.
44 Hu Y, Xie C, Yang H, *et al*. Assessment of Intratumoral and Peritumoral Computed Tomography Radiomics for Predicting Pathological Complete Response to Neoadjuvant Chemoradiation in Patients With Esophageal Squamous Cell Carcinoma. *JAMA Netw Open* 2020;3:e2015927.
45 Chen M, Lu H, Copley SJ, *et al*. A Novel Radiogenomics Biomarker for Predicting Treatment Response and Pneumotoxicity From Programmed Cell Death Protein or Ligand-1 Inhibition Immunotherapy in NSCLC. *J Thorac Oncol* 2023;18:718–30.